View metadata, citation and similar papers at core.ac.uk
brought to you by CORE
provided by Elsevier - Publisher Connector

Crystallization Screens: Compatibility with the Lipidic Cubic Phase for *in Meso* Crystallization of Membrane Proteins

Vadim Cherezov, Hannan Fersi, and Martin Caffrey
Biochemistry, Biophysics, and Chemistry, The Ohio State University, Columbus, Ohio 43210 USA

ABSTRACT The *in meso* method for growing crystals of membrane proteins uses a spontaneously forming lipidic cubic mesophase. The detergent-solubilized protein is dispersed with lipid, typically monoolein, and in so doing the cubic phase self-assembles. A precipitant is added to trigger crystal nucleation and growth. The commercial screen solution series are convenient for use in crystallization trials. The aim of this study was to determine which of the Hampton Screen and Screen 2 series of solutions are compatible with the *in meso* method. These screens contain components any of which could destroy the cubic phase. X-ray diffraction was used for phase identification and for microstructure characterization. The study was done at 4°C and at 20°C. Two types of sample preparations were examined. One used an excess of half-strength screen solution (Prep. 1). The other used a limiting quantity of undiluted screen solution (Prep. 2). At 20°C, over 90% of the screen solutions produced the cubic phase with Prep. 1. This figure dropped to 50% with Prep. 2. In contrast, 50 to 60% of the screens were cubic phase compatible at 4°C under Prep. 1 conditions. The figure fell to 25% with Prep. 2. The mode of action of the diverse screen components are explained on the basis of the phase properties of the monoolein/water system.

INTRODUCTION

One of the rate-limiting steps in determining macromolecular structure by means of diffraction is the preparation of suitable quality crystals (McPherson, 1999). This is particularly true in the case of membrane proteins in which the number of crystallization strategies available is remarkably few. A novel approach for growing crystals of membrane proteins has been reported which makes use of the lipidic cubic mesophase (Fig. 1) (Landau and Rosenbusch, 1996). It has been used to grow diffraction quality crystals of several membrane proteins (Landau and Rosenbusch, 1996; Kolbe et al., 2000; Saas et al., 2000; Luecke et al., 1999).

The prospect exists that the method has general applicability and that it will provide an additional route leading to more membrane protein structures. As with all crystallization studies, however, there is an element of randomness about it because the mechanism of *in meso* crystallization is still unclear (Caffrey, 2000). Accordingly, the multidimensional space in which crystallization occurs must be probed, and this is generally done on an empirical basis. The space referred to encompasses, at a minimum, the physical and chemical environments within which crystallization takes place. The former refers to temperature, pressure, and gravity. The latter deals mainly with concentration and type of solutes and solvents in the system. Crystallization trials involve exploring this multifaceted space in as systematic and efficient a way as possible. Such trials have benefited from a range of screen solutions developed in different laboratories that were designed to sample, with a fine or coarse grid, the relevant crystallization space. A relatively standard crystallization procedure involves mixing the protein of interest in a suitable buffer with an equal volume of screen solution and allowing it, in the form of a hanging or sitting drop, to equilibrate with the undiluted screen solution via the vapor phase (McPherson, 1999). The hope is that during the equilibration period the protein solution passes through a condition favoring crystal nucleation to one supporting the growth of a few large and well-ordered crystals.

The *in meso* method for growing crystals of membrane proteins involves dispersing the protein solution/suspension with a dry lipid, most commonly the monoacylglycerol, monoolein. By referring to the temperature-composition phase diagram for the monoolein/water system (Fig. 2; Qiu and Caffrey, 2000), we know that the very act of mixing the two components, when carried out in the proper ratio at a suitable temperature, leads to spontaneous cubic phase formation. Presumably in the process, the protein is reconstituted into the lipid bilayers that make up the cubic phase (Caffrey, 2000). A precipitant is then added, which triggers crystal nucleation and growth. Salts, such as sodium/potassium phosphate, and sodium chloride, have proved useful in this regard (Landau and Rosenbusch, 1996; Kolbe et al., 2000).

As the *in meso* method is applied to other proteins, a wide range of precipitants in combination with other additives will have to be tested. One potential problem with this has to do with the compatibility of these so-called screening solutions with the cubic phase upon which the method is based. Thus, any component in the screen that destroys the cubic phase may render that particular screen useless. The purpose of the current study is to evaluate the compatibility of the commercially available Hampton Screen and Hampton Screen 2 series (Hampton Research Inc.) with the cubic phase. The Hampton screening kits consist of 50 and 48 solutions, respectively. The solutions themselves are composed of buffers, salts, and precipitants (Fig. 3) in combi-

Received for publication 28 November 2000 and in final form 4 April 2001.

Address reprint requests to Dr. Martin Caffrey, The Ohio State University, 120 W. 18th Avenue, Columbus, OH 43210. Tel: 614-292-8431; Fax: 614-292-1532; E-mail: caffrey.1@osu.edu.

© 2001 by the Biophysical Society

0006-3495/01/07/225/18 $2.00

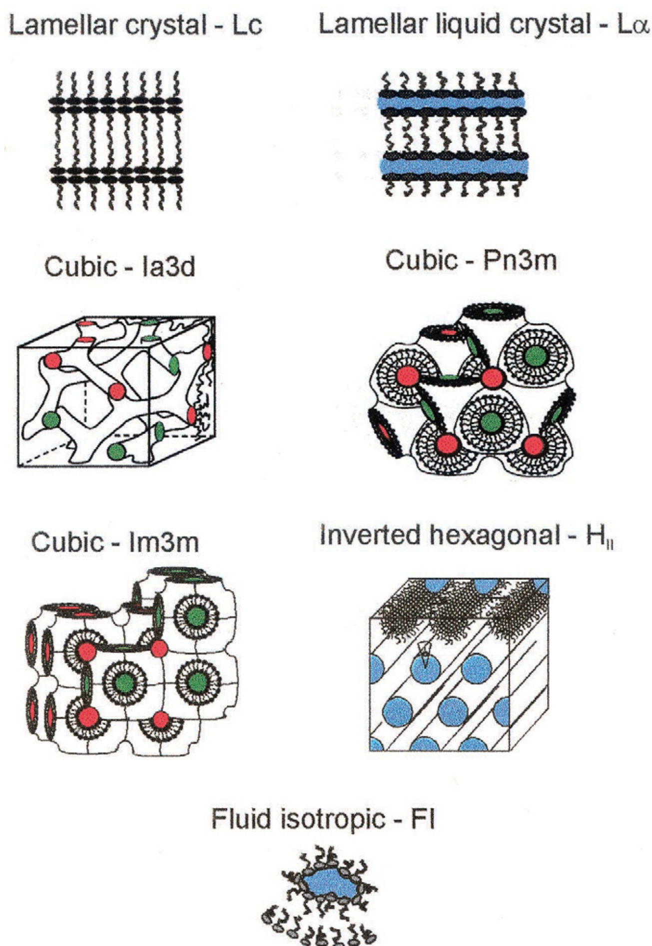

FIGURE 1 Lipid phases. Cartoon representation of the various solid (lamellar crystal phase), mesophase (lamellar liquid crystal phase; cubic-Pn3m phase (space group number 224); cubic-Ia3d phase (space group number 230); cubic-Im3m phase (space group number 229); inverted hexagonal phase), and liquid (fluid isotropic phase (Larsson; 1994) states adopted by lipids dispersed in water. Individual lipids are shown as lollipop figures with the pop and stick parts representing the polar headgroup and the apolar acyl chain, respectively. The colored regions represent water.

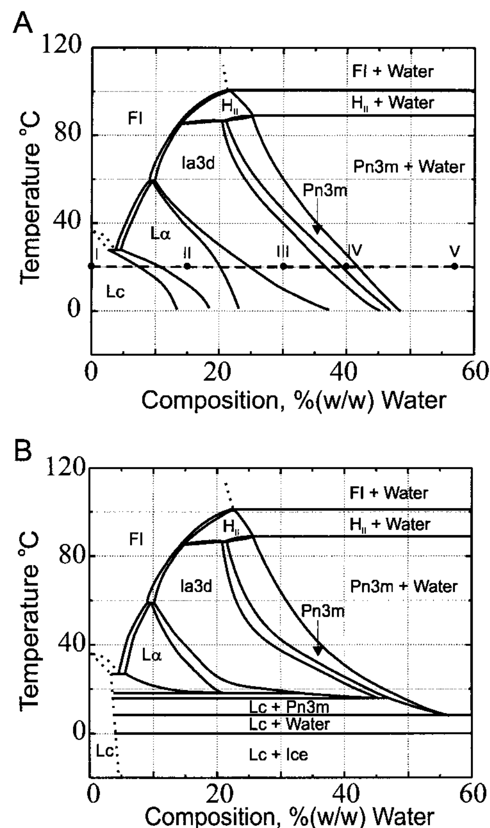

FIGURE 2 Temperature-composition phase diagram for the monoolein/water system. (*A*) Metastable phase diagram (Briggs et al., 1996). (*B*) Equilibrium phase diagram (Qiu and Caffrey; 2000). In *A*, points along the 20°C isotherm identified by roman numerals are referred to in the text. Equilibrium phase diagram (*B*) was constructed in heating direction after resetting samples into the L_c phase by incubation at −15°C.

nations that have proved successful in producing crystals of soluble macromolecules. They are also being used as a starting point for crystallization trials of membrane proteins.

The *in meso* compatibility tests were performed based on protocols currently used in crystallization trials in our lab. The first approach follows the supplier's recommendation of using the screen solutions at half strength. Thus, the diluted screen is mixed with lipid in the ratio monoolein: solution, 43:57 (by weight). According to the monoolein/water phase diagram, a mixture consisting of 43% (w/w) monoolein and 57% (w/w) water at 20°C will produce the cubic-Pn3m phase in equilibrium with excess water (Point V in Fig. 2 *A*). In other words, the cubic phase is fully hydrated and saturated with water under these conditions because the excess water boundary is located at *ca.* 40% (w/w) water. The second approach involves preparing a 2:3 (by weight) mixture of the undiluted screen solution and monoolein. According to Fig. 2 *A* (Point IV), such a combination will produce a cubic phase that is less than fully hydrated at 20°C.

Low- and wide-angle x-ray diffraction were used for phase identification and for phase microstructure characterization. Measurements were made at 4°C and at 20°C. This covers the temperature range in which most crystallization trials are conducted (McPherson, 1999). The phases identified in the course of the study include the solid lamellar crystal (L_c) phase, the liquid fluid isotropic (FI) phase, and five liquid crystal phases: the lamellar liquid crystal (L_α), the cubic-Ia3d, the cubic-Pn3m, the cubic-Im3m, and the inverted hexagonal (H_{II}). Cartoon representations of these phases are presented in Fig. 1. The data show that while most of the screens are compatible with the cubic phase at 20°C, at the lower temperature, and particularly under conditions in which the undiluted screen solutions are used, the cubic phase is no longer stable. Reasons for the instability are discussed in the context of the phase behavior of the monoolein/water system.

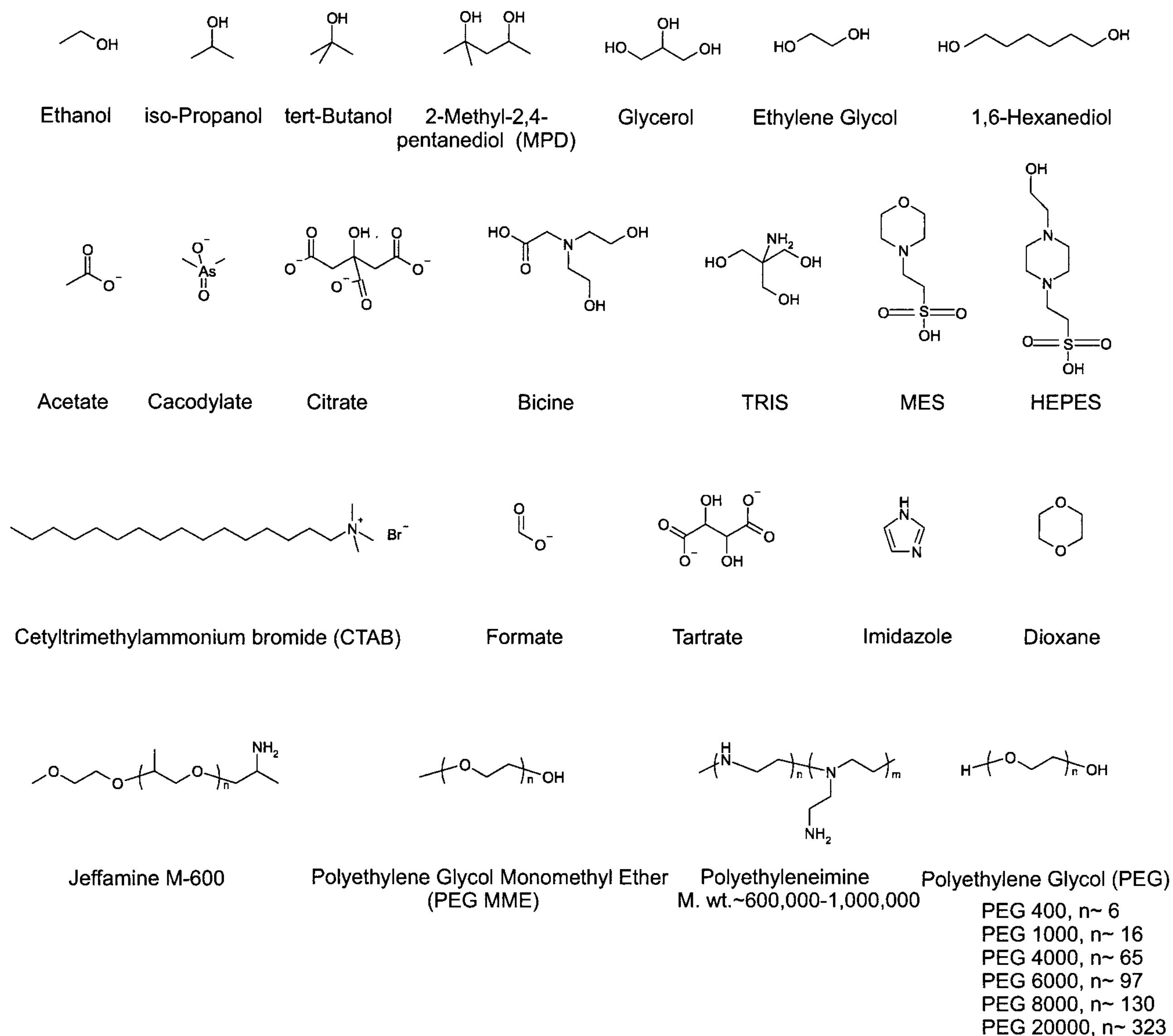

FIGURE 3 Molecular structures of the organic screen components.

MATERIALS AND METHODS

Materials

Monoolein was purchased from Nu Check Prep Inc. (Elysian, MN). It had a reported purity in excess of 99% and was used as supplied. Thin layer chromatography of fresh monoolein was used to verify purity. For this purpose 1, 5, 50, and 200 μg samples of monoolein, dissolved in chloroform, were run on Adsorbosil Plus plates (Alltech, Deerfield, IL) using three different solvent systems: chloroform/acetone (96/4, v/v), chloroform/acetone/methanol/acetic acid (73.5/25/1/0.5 v/v) and hexane/toluene/acetic acid (70/30/1 v/v). The plates were pre-run twice in chloroform/methanol (10/1, v/v). Spots were visualized by spraying with 4.2 M sulfuric acid followed by charring on a hot plate (250°C). Estimated purity of the lipid was in excess of 99.5%. Crystal Screen (hereafter referred to as Screen 1, lot 04169940) and Crystal Screen 2 (Screen 2, lot 05039921) were provided by Hampton Research Inc. (Laguna Niguel, CA). Water (resistivity, >18 MΩ·cm) was purified by using a Milli-Q Water System (Millipore Corporation, Bedford, MA) consisting of a carbon filter cartridge, two ion exchange filter cartridges, and an organic removal cartridge.

Methods

Sample preparation

Samples of fixed composition consisting of monoolein, Hampton Screen solution and water were prepared gravimetrically and transferred to x-ray capillaries using a mechanical mixing device as described (Cheng et al., 1998). Mixing was carried out at room temperature (~22°C), and samples were incubated for different periods of time at 20 or 3°C before being used in diffraction measurements. Long-term stability of hydrated monoolein (40% (w/w) water) was measured using thin layer chromatography as described above. The sample was incubated at 20°C for one and a half months. A small amount of breakdown occurred in this period as evidenced by an impurity level of ~1.5%.

Two types of samples were used in the course of this study. The first (Prep. 1) involved dispersing monoolein with a 1:1 (v/v) dilution of Hampton Screen solution in water. The final concentrations in Prep. 1 were 43% (w/w) monoolein and 57% (w/w) aqueous solution. The second sample preparation type (Prep. 2) combined 60% (w/w) monoolein and 40% (w/w) undiluted screen solution. For both Prep. 1 and 2, ~20 mg monoolein was used in the preparation of each sample. Most of the samples were prepared and fully analyzed in duplicate. The estimated error on sample composition is ±3% (w/w) monoolein.

X-ray diffraction

Low- and wide-angle x-ray diffraction patterns were recorded in groups of seven on image plates (Fuji HR-IIIn, Fuji Medical Systems U.S.A., Stamford, CT) using an 18 kW rotating anode x-ray source (Rigaku RU-300, Rigaku U.S.A., Danvers, MA) and a low-angle camera as described (Qiu and Caffrey, 2000). The sample-to-detector distance was usually either 26 or 34 cm. Immediately upon preparation, samples were incubated for at least 1 day at room temperature (20 to 22°C). They were then placed in a temperature-regulated holder, designed to accommodate seven samples (Briggs et al., 1996), at 20°C and were used immediately in x-ray diffraction measurement at this temperature. After data collection at 20°C, the samples were placed in a refrigerator at 3°C for a three- to four-week period. Just before the diffraction measurement, the samples were transferred from the refrigerator at 3°C into the sample holder in a walk-in refrigerator at 4°C. The holder containing the samples was then placed on ice and transferred to the x-ray machine. This last step took no more than a few minutes. Measurements were made at 4°C following preincubation at this temperature for at least 1 h. Exposure times of 30 min were usually used at both 4 and 20°C. Diffraction patterns were processed and analyzed as described previously (Ai and Caffrey, 2000). This provided information on phase microstructure and phase identity based on an indexing of the low-angle reflections and the nature of the scattering and/or diffraction behavior at wide-angles.

A few diffraction patterns were collected on beamline ID-2 at the European Synchrotron Radiation Facility (ESRF, Grenoble, France) some of which are shown in Fig. 4 (patterns G–I). The same conditions as described above for measurements on the rotating anode x-ray source were used at the ESRF.

RESULTS

The study involved recording and analyzing the diffraction patterns for monoolein samples dispersed with Hampton Screen solutions in diluted (Prep. 1) or undiluted form (Prep. 2) at 4 and 20°C. Representative diffraction patterns are shown in Fig. 4. The results are summarized in Table 1 in which the phase type and corresponding lattice parameters are reported. The identity, concentration, and pH of the components (precipitant, salt, and buffer) used to prepare the Screen solutions as specified by the supplier are included in the table. The data are arranged in Table 1 by phase type. The sequence of phases generally matches that seen in the phase diagram (Fig. 2) with increasing hydration and temperature in the following order: FI, L_c, L_α, cubic-Ia3d, cubic-Pn3m, cubic-Im3m, and H_{II}. Within a given phase, entries are arranged by structure parameter size in Table 1. Phase coexistence is apparent when multiple

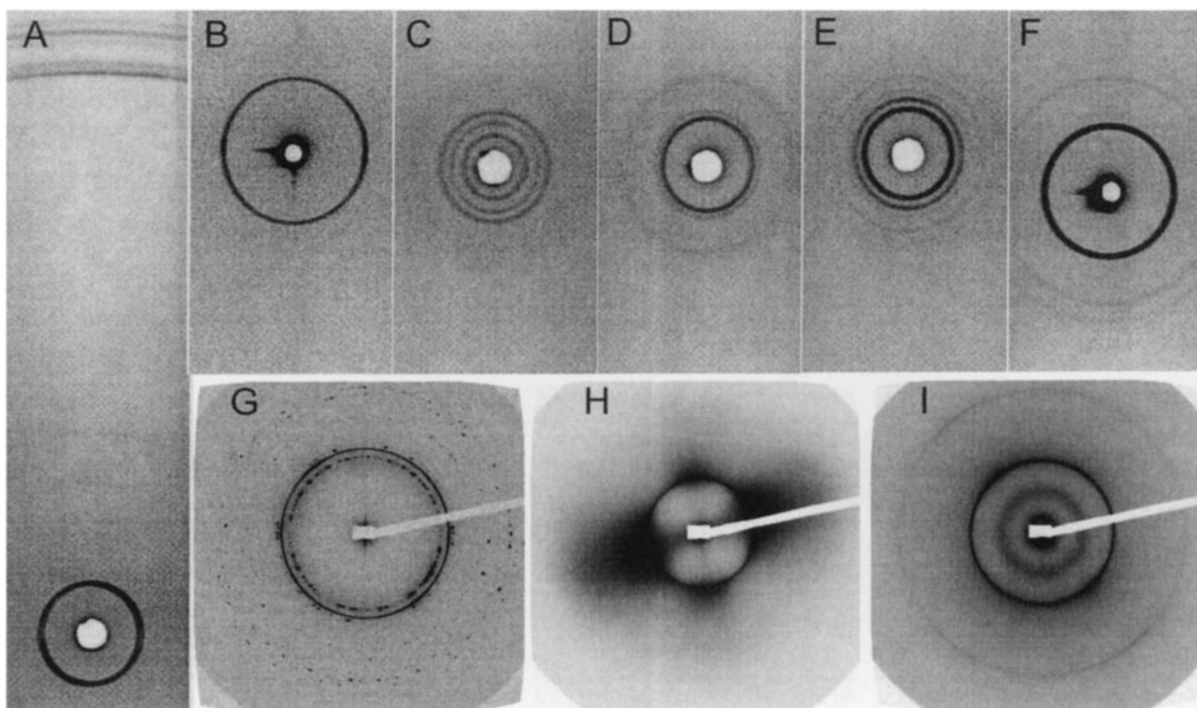

FIGURE 4 X-ray diffraction patterns of the various phases identified in the monoolein/screen solution/water system. Data were collected on a rotating anode x-ray source or at the ESRF as described in Materials and Methods. Sample (see Table 1 for composition, preparation type, measurement temperature) and phase identity follow: (*A*) 1–10.2.4, L_c phase. (*B*) 1–41.2.20, L_α phase. (*C*) 2–45.1.4, cubic-Im3m phase. (*D*) 2–1.1.4, cubic-Ia3d phase. (*E*) 2–6.1.4, cubic-Pn3m phase. (*F*) 2–32.2.20, H_{II} phase. (*G*) 1–45.2.20, L_α and cubic-Ia3d phase coexistence. The cubic phase pattern is spotty. (*H*) 2–43.1.20, L_α phase in conjunction with extensive diffuse scattering. (*I*) 1–1.1.20, L_α phase and disordered cubic (inner diffuse ring) phase coexistence.

TABLE 1. Effect of Hampton Screen solutions on the phase properties and phase microstructure of the monoolein/water system at 4 °C and 20 °C

Screen1, Prep.1, 20 °C

Code	Crystal screen solution no.	Screen composition *							Phase identification and structure parameter (Å)							Footnotes
		Precipitant		Salt		Buffer										
		Concentration	Identity	Concentration	Identity	Concentration	Identity	pH	FI	L_c d_{001}	L_α d_{001}	cubic-Ia3d d_{100}	cubic-Pn3m d_{100}	cubic-Im3m d_{100}	H_{II} d_{10}	
1-40.1.20	40	20% 20%	Isopropanol PEG 4000			0.1 M	Na citrate	5.6			44.9					
1-41.1.20	41	10% 20%	Isopropanol PEG 4000			0.1 M	HEPES	7.5			45.8					†
1-5.1.20	5	30%	MPD	0.2 M	Na citrate	0.1 M	HEPES	7.5			48	206				‡, §
1-26.1.20	26	30%	MPD	0.2 M	Ammonium acetate	0.1 M	Na citrate	5.6			49.2	204				‡, §
1-21.1.20	21	30%	MPD	0.2 M	Mg acetate	0.1 M	Na cacodylate	6.5			49.5	199	(128)			‡, §, ‖
1-1.1.20	1	30%	MPD	0.02 M	Ca chloride	0.1 M	Na acetate	4.6			49.9	230				‡, §
1-17.1.20	17	30%	PEG 4000	0.2 M	Li sulfate	0.1 M	Tris	8.5				127				†
1-22.1.20	22	30%	PEG 4000	0.2 M	Na acetate	0.1 M	Tris	8.5				127				†
1-6.1.20	6	30%	PEG 4000	0.2 M	Mg chloride	0.1 M	Tris	8.5				128				†
1-28.1.20	28	30%	PEG 8000	0.2 M	Na acetate	0.1 M	Na cacodylate	6.5				128				†
1-10.1.20	10	30%	PEG 4000	0.2 M	Ammonium acetate	0.1 M	Na acetate	4.6				128				†
1-9.1.20	9	30%	PEG 4000	0.2 M	Ammonium acetate	0.1 M	Na citrate	5.6				130				†
1-30.1.20	30	30%	PEG 8000	0.2 M	Ammonium sulfate							130				†
1-31.1.20	31	30%	PEG 4000	0.2 M	Ammonium sulfate							130				†
1-15.1.20	15	30%	PEG 8000	0.2 M	Ammonium sulfate	0.1 M	Na cacodylate	6.5				130				†
1-20.1.20	20	25%	PEG 4000	0.2 M	Ammonium sulfate	0.1 M	Na acetate	4.6				135				†
1-18.1.20	18	20%	PEG 8000	0.2 M	Mg acetate	0.1 M	Na cacodylate	6.5				138				†
1-42.1.20	42	20%	PEG 8000	0.05 M	K phosphate							139				†
1-46.1.20	46	18%	PEG 8000	0.2 M	Ca acetate	0.1 M	Na cacodylate	6.5				141				†
1-45.1.20	45	18%	PEG 8000	0.2 M	Zn acetate	0.1 M	Na cacodylate	6.5				142				†
1-50.1.20	50	15%	PEG 8000	0.5 M	Li sulfate							145				
1-37.1.20	37	8%	PEG 4000			0.1 M	Na acetate	4.6				153				†
1-36.1.20	36	8%	PEG 8000			0.1 M	Tris	8.5				156				
1-38.1.20	38	1.4 M	Na citrate			0.1 M	HEPES	7.5					87			†
1-4.1.20	4	2 M	Ammonium sulfate			0.1 M	Tris	8.5					91			†
1-16.1.20	16	1.5 M	Li sulfate			0.1 M	HEPES	7.5					91			†
1-39.1.20	39	2% 2 M	PEG 400 Ammonium sulfate			0.1 M	HEPES	7.5					92			†
1-32.1.20	32	2 M	Ammonium sulfate										92			†
1-47.1.20	47	2 M	Ammonium sulfate			0.1 M	Na acetate	4.6					93			†
1-43.1.20	43	30%	PEG 1500										95			†
1-33.1.20	33	4 M	Na formate										96			
1-35.1.20	35	1.6 M	Na, K phosphate			0.1 M	HEPES	7.5					96			†
1-49.1.20	49	2%	PEG 8000	1 M	Li sulfate								96			
1-48.1.20	48	2 M	Ammonium phosphate			0.1 M	Tris	8.5					97			†
1-29.1.20	29	0.8 M	K, Na tartrate			0.1 M	HEPES	7.5					98			
1-13.1.20	13	30%	PEG 400	0.2 M	Na citrate	0.1 M	Tris	8.5					98			†
1-11.1.20	11	1 M	Ammonium phosphate			0.1 M	Na citrate	5.6					101			†
1-34.1.20	34	2 M	Na formate			0.1 M	Na acetate	4.6					101			†
1-23.1.20	23	30%	PEG 400	0.2 M	Mg chloride	0.1 M	HEPES	7.5					101			†
1-14.1.20	14	28%	PEG 400	0.2 M	Ca chloride	0.1 M	HEPES	7.5					102			†
1-7.1.20	7	1.4 M	Na acetate			0.1 M	Na cacodylate	6.5					102			†
1-2.1.20	2	0.4 M	K, Na tartrate										104			†
1-25.1.20	25	1 M	Na acetate			0.1 M	Imidazole	6.5					104			†
1-3.1.20	3	0.4 M	Ammonium phosphate										106			†
1-44.1.20	44	0.2 M	Mg formate										106			†
0.1.20	**0**												**107**			**†**
1-27.1.20	27	20%	Isopropanol	0.2 M	Na citrate	0.1 M	HEPES	7.5					116			†, ‡
1-19.1.20	19	30%	Isopropanol	0.2 M	Ammonium acetate	0.1 M	Tris	8.5					118			†, ‡
1-12.1.20	12	30%	Isopropanol	0.2 M	Mg chloride	0.1 M	HEPES	7.5					118			†, ‡
1-8.1.20	8	30%	Isopropanol	0.2 M	Na citrate	0.1 M	Na cacodylate	6.5					119			†, ‡
1-24.1.20	24	20%	Isopropanol	0.2 M	Ca chloride	0.1 M	Na acetate	4.6					122			†, ‡

TABLE 1.—*Continued*

Screen 2, Prep. 1, 20 °C

Code	Crystal screen solution no.	Screen composition*								Phase identification and structure parameter (Å)							Footnotes
		Precipitant			Salt		Buffer										
		Concentration	Identity	pH	Concentration	Identity	Concentration	Identity	pH	FI	L_c d_{001}	L_α d_{001}	cubic-Ia3d d_{100}	cubic-Pn3m d_{100}	cubic-Im3m d_{100}	H_{II} d_{10}	
2-10.1.20	10	30%	MPD		0.2 M	Na chloride	0.1 M	Na acetate	4.6			50.4	207				§
2-19.1.20	19	2.5 M	1,6 Hexanediol				0.1 M	Na citrate	5.6			52.3					
2-43.1.20	43	50%	MPD		0.2 M	Ammonium phosphate	0.1 M	Tris	8.5			68					¶
2-39.1.20	39	3.4 M	1,6 Hexanediol		0.2 M	Mg chloride	0.1 M	Tris	8.5			69					§, ¶
2-26.1.20	26	30%	PEG MME 5000		0.2 M	Ammonium sulfate	0.1 M	MES	6.5				128				†
2-38.1.20	38	20%	PEG 10,000				0.1 M	HEPES	7.5				138				
2-7.1.20	7	10% 10%	PEG 1000 PEG 8000										147				
2-37.1.20	37	10% 8%	PEG 8000 Ethylene Glycol				0.1 M	HEPES	7.5				149				
2-22.1.20	22	12%	PEG 20,000				0.1 M	MES	6.5				151				
2-30.1.20	30	10% 5%	PEG 6000 MPD				0.1 M	HEPES	7.5				151				
2-48.1.20	48	10%	PEG 20,000		2%	Dioxane	0.1 M	Bicine	9				152				
2-3.1.20	3	25%	Ethylene Glycol										155				
2-17.1.20	17	35%	tert-Butanol				0.1 M	Na citrate	5.6				177	115			‡, §
2-40.1.20	40	25%	tert-Butanol		0.1 M	Ca chloride	0.1 M	Tris	8.5				183	117			‡, §
2-29.1.20	29	30%	MPD		0.5 M	Ammonium sulfate	0.1 M	HEPES	7.5				200	127			‡, §
2-24.1.20	24	30%	Jeffamine M-600		0.05 M	Cs chloride	0.1 M	MES	6.5				209				‡, §
2-42.1.20	42	12%	Glycerol		1.5 M	Ammonium sulfate	0.1 M	Tris	8.5					85			
2-28.1.20	28	1.6 M	Na citrate	6.5										87			†
2-14.1.20	14	2 M	Ammonium sulfate		0.2 M	K, Na tartrate	0.1 M	Na citrate	5.6					90			
2-32.1.20	32	1.6 M	Ammonium sulfate		0.1 M	Na chloride	0.1 M	HEPES	7.5					91			
2-36.1.20	36	4.3 M	Na chloride				0.1 M	HEPES	7.5					91			
2-20.1.20	20	1.6 M	Mg sulfate				0.1 M	MES	6.5					91			
2-41.1.20	41	1M	Li sulfate		0.01 M	Ni chloride	0.1 M	Tris	8.5					91			
2-15.1.20	15	1M	Li sulfate		0.5 M	Ammonium sulfate	0.1 M	Na citrate	5.6					92			
2-13.1.20	13	30%	PEG MME 2000		0.2 M	Ammonium sulfate	0.1 M	Na acetate	4.6					92			
2-1.1.20	1	10%	PEG 6000		2 M	Na chloride								93			
2-47.1.20	47	2 M	Mg chloride				0.1 M	Bicine	9					93			
2-25.1.20	25	1.8 M	Ammonium sulfate		0.01 M	Co chloride	0.1 M	MES	6.5					94			
2-5.1.20	5	5%	Isopropanol		2 M	Ammonium sulfate								94			
2-45.1.20	45	20%	PEG MME 2000		0.01 M	Ni chloride	0.1 M	Tris	8.5					95			
2-23.1.20	23	10%	Dioxane		1.6 M	Ammonium sulfate	0.1 M	MES	6.5					96			
2-34.1.20	34	1 M	Na acetate		0.05 M	Cd sulfate	0.1 M	HEPES	7.5					100			
2-33.1.20	33	2 M	Ammonium formate				0.1 M	HEPES	7.5					100			
2-21.1.20	21	2 M	Na chloride		0.2 M	Na, K phosphate	0.1 M	MES	6.5					100			
2-9.1.20	9	2 M	Na chloride				0.1 M	Na acetate	4.6					102			
2-12.1.20	12	30%	PEG 400		0.1 M	Cd chloride	0.1 M	Na acetate	4.6					102			
2-46.1.20	46	30%	PEG MME 550		0.1 M	Na chloride	0.1 M	Bicine	9					104			
2-27.1.20	27	25%	PEG MME 550		0.01 M	Zn sulfate	0.1 M	MES	6.5					105			
2-2.1.20	2	0.01M 0.5 M	Mg chloride Na chloride		0.01 M	CTAB								105			
2-16.1.20	16	4%	Polyethyleneimine		0.5 M	Na chloride	0.1 M	Na citrate	5.6					106			
0.1.20	**0**													**107**			†
2-8.1.20	8	10%	Ethanol		1.5 M	Na chloride								109			
2-6.1.20	6	1 M	Imidazole	7										113			
2-44.1.20	44	20%	Ethanol				0.1 M	Tris	8.5					118			
2-18.1.20	18	10%	Jeffamine M-600		0.01 M	Fe chloride	0.1 M	Na citrate	5.6					121			‡
2-11.1.20	11	1 M	1,6 Hexanediol		0.01 M	Co chloride	0.1 M	Na acetate	4.6					125			
2-31.1.20	31	20%	Jeffamine M-600				0.1 M	HEPES	7.5					126			†, ‡
2-4.1.20	4	35%	Dioxane											130			‡
2-35.1.20	35	70%	MPD				0.1 M	HEPES	7.5								#

TABLE 1.—*Continued*

Screen 1, Prep. 2, 20 °C

Code	Crystal screen solution no.	Screen composition* Precipitant Concen-tration	Precipitant Identity	Salt Concen-tration	Salt Identity	Buffer Concen-tration	Buffer Identity	pH	Phase identification and structure parameter (Å) FI	L_c d_{001}	L_α d_{001}	cubic-Ia3d d_{100}	cubic-Pn3m d_{100}	cubic-Im3m d_{100}	H_{II} d_{10}	Footnotes
1-40.2.20	40	20% 20%	Isopropanol PEG 4000			0.1 M	Na citrate	5.6			40.5					
1-41.2.20	41	10% 20%	Isopropanol PEG 4000			0.1 M	HEPES	7.5			41.5					†
1-5.2.20	5	30%	MPD	0.2 M	Na citrate	0.1 M	HEPES	7.5			41.6					
1-8.2.20	8	30%	Isopropanol	0.2 M	Na citrate	0.1 M	Na cacodylate	6.5			42	142				‡, §
1-28.2.20	28	30%	PEG 8000	0.2 M	Na acetate	0.1 M	Na cacodylate	6.5			42.3			117		‡
1-10.2.20	10	30%	PEG 4000	0.2 M	Ammonium acetate	0.1 M	Na acetate	4.6			42.5			122		‡
1-43.2.20	43	30%	PEG 1500								43.2					†
1-45.2.20	45	18%	PEG 8000	0.2 M	Zn acetate	0.1 M	Na cacodylate	6.5			43.8	118				†
1-42.2.20	42	20%	PEG 8000	0.05 M	K phosphate						44.1					†
1-17.2.20	17	30%	PEG 4000	0.2 M	Li sulfate	0.1 M	Tris	8.5			44.5			112		
1-12.2.20	12	30%	Isopropanol	0.2 M	Mg chloride	0.1 M	HEPES	7.5			45.8					
1-27.2.20	27	20%	Isopropanol	0.2 M	Na citrate	0.1 M	HEPES	7.5			46.2					
1-26.2.20	26	30%	MPD	0.2 M	Ammonium acetate	0.1 M	Na citrate	5.6			46.5					
1-21.2.20	21	30%	MPD	0.2 M	Mg acetate	0.1 M	Na cacodylate	6.5			46.8					
1-19.2.20	19	30%	Isopropanol	0.2 M	Ammonium acetate	0.1 M	Tris	8.5			47.9					
1-1.2.20	1	30%	MPD	0.02 M	Ca chloride	0.1 M	Na acetate	4.6			48.7					
1-24.2.20	24	20%	Isopropanol	0.2 M	Ca chloride	0.1 M	Na acetate	4.6			49	174				‡, §
1-22.2.20	22	30%	PEG 4000	0.2 M	Na acetate	0.1 M	Tris	8.5				104				‡
1-6.2.20	6	30%	PEG 4000	0.2 M	Mg chloride	0.1 M	Tris	8.5				106				‡
1-30.2.20	30	30%	PEG 8000	0.2 M	Ammonium sulfate							114				
1-15.2.20	15	30%	PEG 8000	0.2 M	Ammonium sulfate	0.1 M	Na cacodylate	6.5				115				‡
1-18.2.20	18	20%	PEG 8000	0.2 M	Mg acetate	0.1 M	Na cacodylate	6.5				116				
1-20.2.20	20	25%	PEG 4000	0.2 M	Ammonium sulfate	0.1 M	Na acetate	4.6				118				
1-46.2.20	46	18%	PEG 8000	0.2 M	Ca acetate	0.1 M	Na cacodylate	6.5				119				
1-36.2.20	36	8%	PEG 8000			0.1 M	Tris	8.5				120				
1-50.2.20	50	15%	PEG 8000	0.5 M	Li sulfate							128				
1-37.2.20	37	8%	PEG 4000			0.1 M	Na acetate	4.6				132				
1-13.2.20	13	30%	PEG 400	0.2 M	Na citrate	0.1 M	Tris	8.5				144	88			‡
1-49.2.20	49	2%	PEG 8000	1 M	Li sulfate								83			
1-35.2.20	35	1.6 M	Na, K phosphate			0.1 M	HEPES	7.5					85			†
1-48.2.20	48	2 M	Ammonium phosphate			0.1 M	Tirs	8.5					86			†
1-29.2.20	29	0.8 M	K, Na tartrate			0.1 M	HEPES	7.5					87			†
1-33.2.20	33	4 M	Na formate										87			
1-7.2.20	7	1.4 M	Na acetate			0.1 M	Na cacodylate	6.5					93			
1-11.2.20	11	1 M	Ammonium phosphate			0.1 M	Na citrate	5.6					94			
1-34.2.20	34	2 M	Na formate			0.1 M	Na acetate	4.6					95			
1-14.2.20	14	28%	PEG 400	0.2 M	Ca chloride	0.1 M	HEPES	7.5					96			‡
1-25.2.20	25	1 M	Na acetate			0.1 M	Imidazole	6.5					97			
1-23.2.20	23	30%	PEG 400	0.2 M	Mg chloride	0.1 M	HEPES	7.5					98			‡
1-3.2.20	3	0.4 M	Ammonium phosphate										98			
1-2.2.20	2	0.4 M	K, Na tartrate										99			
1-44.2.20	44	0.2 M	Mg formate										99			
0.2.20	**0**												**102**			†
1-31.2.20	31	30%	PEG 4000	0.2 M	Ammonium sulfate									112		
1-9.2.20	9	30%	PEG 4000	0.2 M	Ammonium acetate	0.1 M	Na citrate	5.6						118		‡
1-4.2.20	4	2 M	Ammonium sulfate			0.1 M	Tris	8.5							47.8	
1-38.2.20	38	1.4 M	Na citrate			0.1 M	HEPES	7.5							49.2	
1-16.2.20	16	1.5 M	Li sulfate			0.1 M	HEPES	7.5							50.3	
1-39.2.20	39	2% 2 M	PEG 400 Ammonium sulfate			0.1 M	HEPES	7.5							50.3	
1-32.2.20	32	2 M	Ammonium sulfate												52.6	†
1-47.2.20	47	2 M	Ammonium sulfate			0.1 M	Na acetate	4.6							52.8	

TABLE 1.—*Continued*

Screen 2, Prep. 2, 20 °C

Code	Crystal screen solution no.	Screen composition* Precipitant Concentration	Precipitant Identity	Precipitant pH	Salt Concentration	Salt Identity	Buffer Concentration	Buffer Identity	Buffer pH	Phase identification and structure parameter (Å) FI	L_c d_{001}	L_α d_{001}	cubic-Ia3d d_{100}	cubic-Pn3m d_{100}	cubic-Im3m d_{100}	H_{II} d_{10}	Footnotes
2-35.2.20	35	70%	MPD				0.1 M	HEPES	7.5	35.1							†
2-43.2.20	43	50%	MPD		0.2 M	Ammonium phosphate	0.1 M	Tris	8.5			41.1					¶
2-29.2.20	29	30%	MPD		0.5 M	Ammonium sulfate	0.1 M	HEPES	7.5			41.4					†
2-38.2.20	38	20%	PEG 10,000				0.1 M	HEPES	7.5			43.5					
2-7.2.20	7	10% 10%	PEG 1000 PEG 8000									44					
2-17.2.20	17	35%	tert-Butanol				0.1 M	Na citrate	5.6			44					
2-30.2.20	30	10% 5%	PEG 6000 MPD				0.1 M	HEPES	7.5			45.1					
2-22.2.20	22	12%	PEG 20,000				0.1 M	MES	6.5			45.2	126				
2-40.2.20	40	25%	tert-Butanol		0.1 M	Ca chloride	0.1 M	Tris	8.5			46.3	155				
2-39.2.20	39	3.4 M	1,6 Hexanediol		0.2 M	Mg chloride	0.1 M	Tris	8.5			46.9					
2-10.2.20	10	30%	MPD		0.2 M	Na chloride	0.1 M	Na acetate	4.6			47					
2-24.2.20	24	30%	Jeffamine M-600		0.05 M	Cs chloride	0.1 M	MES	6.5			49					
2-4.2.20	4	35%	Dioxane									49.1					
2-19.2.20	19	2.5 M	1,6 Hexanediol				0.1 M	Na citrate	5.6			49.1					
2-11.2.20	11	1 M	1,6 Hexanediol		0.01 M	Co chloride	0.1 M	Na acetate	4.6			50.5					
2-20.2.20	20	1.6 M	Mg sulfate				0.1 M	MES	6.5				113				†
2-47.2.20	47	2 M	Mg chloride				0.1 M	Bicine	9				125				
2-37.2.20	37	10% 8%	PEG 8000 Ethylene glycol				0.1 M	HEPES	7.5				126				
2-1.2.20	1	10%	PEG 6000		2 M	Na chloride							129				
2-44.2.20	44	20%	Ethanol				0.1 M	Tris	8.5				132				‡
2-48.2.20	48	10%	PEG 20,000		2%	Dioxane	0.1 M	Bicine	9				130				
2-16.2.20	16	4%	Polyethyleneimine		0.5 M	Na chloride	0.1 M	Na citrate	5.6				148				
2-8.2.20	8	10%	Ethanol		1.5 M	Na chloride							154				
2-12.2.20	12	30%	PEG 400		0.1 M	Cd chloride	0.1 M	Na acetate	4.6				155	101			
2-3.2.20	3	25%	Ethylene glycol										159				
2-18.2.20	18	10%	Jeffamine M-600		0.01 M	Fe chloride	0.1 M	Na citrate	5.6				159				
2-6.2.20	6	1 M	Imidazole	7									160				
2-5.2.20	5	5%	Isopropanol		2 M	Ammonium sulfate								75			‡
2-23.2.20	23	10%	Dioxane		1.6 M	Ammonium sulfate	0.1 M	MES	6.5					76			‡
2-25.2.20	25	1.8 M	Ammonium sulfate		0.01 M	Co chloride	0.1 M	MES	6.5					80		53.2	
2-45.2.20	45	20%	PEG MME 2000		0.01 M	Ni chloride	0.1 M	Tris	8.5					82			†, ‡
2-46.2.20	46	30%	PEG MME 550		0.1 M	Na chloride	0.1 M	Bicine	9					85			†, ‡
2-36.2.20	36	4.3 M	Na chloride				0.1 M	HEPES	7.5					86			
2-21.2.20	21	2 M	Na chloride		0.2 M	Na, K phosphate	0.1 M	MES	6.5					93			
2-33.2.20	33	2 M	Ammonium formate				0.1 M	HEPES	7.5					93			
2-34.2.20	34	1 M	Na acetate		0.05 M	Cd sulfate	0.1 M	HEPES	7.5					93			
2-9.2.20	9	2 M	Na chloride				0.1 M	Na acetate	4.6					95			
2-27.2.20	27	25%	PEG MME 550		0.01 M	Zn sulfate	0.1 M	MES	6.5					100			
0.2.20	**0**													**102**			**†**
2-2.2.20	2	0.01 M 0.5 M	Mg chloride Na chloride		0.01 M	CTAB								103			
2-31.2.20	31	20%	Jeffamine M-600				0.1 M	HEPES	7.5						114		
2-26.2.20	26	30%	PEG MME 5000		0.2 M	Ammonium sulfate	0.1 M	MES	6.5						116		†, ‡
2-13.2.20	13	30%	PEG MME 2000		0.2 M	Ammonium sulfate	0.1 M	Na acetate	4.6						121		†, ‡
2-42.2.20	42	12%	Glycerol		1.5 M	Ammonium sulfate	0.1 M	Tris	8.5							50.2	
2-28.2.20	28	1.6 M	Na citrate	6.5												50.7	†
2-14.2.20	14	2 M	Ammonium sulfate		0.2 M	K, Na tartrate	0.1 M	Na citrate	5.6							50.8	
2-41.2.20	41	1M	Li sulfate		0.01 M	Ni chloride	0.1 M	Tris	8.5							51.2	†
2-32.2.20	32	1.6 M	Ammonium sulfate		0.1 M	Na chloride	0.1 M	HEPES	7.5							52.1	
2-15.2.20	15	1M	Li sulfate		0.5 M	Ammonium sulfate	0.1 M	Na citrate	5.6							52.2	

TABLE 1.—*Continued*

Screen 1, Prep. 1, 4 °C

Code	Crystal screen solution no.	Screen composition*							Phase identification and structure parameter (Å)							Footnotes
		Precipitant		Salt		Buffer										
		Concentration	Identity	Concentration	Identity	Concentration	Identity	pH	FI	L_c d_{001}	L_α d_{001}	cubic-Ia3d d_{100}	cubic-Pn3m d_{100}	cubic-Im3m d_{100}	H_{II} d_{10}	
1-11.1.4	11	1 M	Ammonium phosphate			0.1 M	Na citrate	5.6		49.3						
1-21.1.4	21	30%	MPD	0.2 M	Mg acetate	0.1 M	Na cacodylate	6.5		49.4			(126)			‖
1-25.1.4	25	1 M	Na acetate			0.1 M	Imidazole	6.5		49.5						
1-8.1.4	8	30%	Isopropanol	0.2 M	Na citrate	0.1 M	Na cacodylate	6.5		49.5		(202)				‖
1-49.1.4	49	2%	PEG 8000	1 M	Li sulfate					49.5						
1-40.1.4	40	20% 20%	Isopropanol PEG 4000			0.1 M	Na citrate	5.6			45.1					
1-28.1.4	28	30%	PEG 8000	0.2 M	Na acetate	0.1 M	Na cacodylate	6.5			46.3					
1-43.1.4	43	30%	PEG 1500							(49.4)	46.4					‖
1-9.1.4	9	30%	PEG 4000	0.2 M	Ammonium acetate	0.1 M	Na citrate	5.6			46.6					
1-10.1.4	10	30%	PEG 4000	0.2 M	Ammonium acetate	0.1 M	Na acetate	4.6			46.6					
1-31.1.4	31	30%	PEG 4000	0.2 M	Ammonium sulfate						46.6					
1-41.1.4	41	10% 20%	Isopropanol PEG 4000			0.1 M	HEPES	7.5			46.6					
1-15.1.4	15	30%	PEG 8000	0.2 M	Ammonium sulfate	0.1 M	Na cacodylate	6.5			46.9					
1-30.1.4	30	30%	PEG 8000	0.2 M	Ammonium sulfate						47					
1-20.1.4	20	25%	PEG 4000	0.2 M	Ammonium sulfate	0.1 M	Na acetate	4.6			47.3					**
1-18.1.4	18	20%	PEG 8000	0.2 M	Mg acetate	0.1 M	Na cacodylate	6.5			47.5					
1-42.1.4	42	20%	PEG 8000	0.05 M	K phosphate						47.8					
1-45.1.4	45	18%	PEG 8000	0.2 M	Zn acetate	0.1 M	Na cacodylate	6.5		(49.3)	47.8					†, ‖
1-46.1.4	46	18%	PEG 8000	0.2 M	Ca acetate	0.1 M	Na cacodylate	6.5			47.9					
1-5.1.4	5	30%	MPD	0.2 M	Na citrate	0.1 M	HEPES	7.5			48.6	203	131			‡
1-26.1.4	26	30%	MPD	0.2 M	Ammonium acetate	0.1 M	Na citrate	5.6			49.1					**
1-37.1.4	37	8%	PEG 4000			0.1 M	Na acetate	4.6			49.5					††
1-1.1.4	1	30%	MPD	0.02 M	Ca chloride	0.1 M	Na acetate	4.6			49.6					¶
1-39.1.4	39	2% 2 M	PEG 400 Ammonium sulfate			0.1 M	HEPES	7.5			49.9		108			
1-17.1.4	17	30%	PEG 4000	0.2 M	Li sulfate	0.1 M	Tris	8.5				127				
1-22.1.4	22	30%	PEG 4000	0.2 M	Na acetate	0.1 M	Tris	8.5				127				
1-6.1.4	6	30%	PEG 4000	0.2 M	Mg chloride	0.1 M	Tris	8.5				128				
1-50.1.4	50	15%	PEG 8000	0.5 M	Li sulfate						(47.3)	151				‖
1-36.1.4	36	8%	PEG 8000			0.1 M	Tris	8.5				158				
1-24.1.4	24	20%	Isopropanol	0.2 M	Ca chloride	0.1 M	Na acetate	4.6				214	137			†, §
1-19.1.4	19	30%	Isopropanol	0.2 M	Ammonium acetate	0.1 M	Tris	8.5			((49.9))	240	(121)			§, ‖
1-13.1.4	13	30%	PEG 400	0.2 M	Na citrate	0.1 M	Tris	8.5					95			†
1-4.1.4	4	2 M	Ammonium sulfate			0.1 M	Tris	8.5					96			
1-16.1.4	16	1.5 M	Li sulfate			0.1 M	HEPES	7.5		(49.4)			98			‖
1-48.1.4	48	2 M	Ammonium phosphate			0.1 M	Tris	8.5					106			
1-47.1.4	47	2 M	Ammonium sulfate			0.1 M	Na acetate	4.6					108			
1-14.1.4	14	28%	PEG 400	0.2 M	Ca chloride	0.1 M	HEPES	7.5					111			
1-32.1.4	32	2 M	Ammonium sulfate										112			
1-23.1.4	23	30%	PEG 400	0.2 M	Mg chloride	0.1 M	HEPES	7.5					113			
1-34.1.4	34	2 M	Na formate			0.1 M	Na acetate	4.6					114			
1-33.1.4	33	4 M	Na formate										114			
1-29.1.4	29	0.8 M	K, Na tartrate			0.1 M	HEPES	7.5					116			
1-7.1.4	7	1.4 M	Na acetate			0.1 M	Na cacodylate	6.5					117			
1-3.1.4	3	0.4 M	Ammonium phosphate										117			
1-35.1.4	35	1.6 M	Na, K phosphate			0.1 M	HEPES	7.5		(49.4)			117			‖
1-2.1.4	2	0.4 M	K, Na tartrate										118			
1-44.1.4	44	0.2 M	Mg formate										118			
0.1.4	**0**												**119**			†
1-27.1.4	27	20%	Isopropanol	0.2 M	Na citrate	0.1 M	HEPES	7.5					126			‡

TABLE 1.—*Continued*

Screen 2, Prep. 1, 4 °C

Code	Crystal screen solution no.	Screen composition*								Phase identification and structure parameter (Å)							Footnotes
		Precipitant			Salt		Buffer										
		Concen-tration	Identity	pH	Concen-tration	Identity	Concen-tration	Identity	pH	FI	L_c d_{001}	L_α d_{001}	cubic-Ia3d d_{100}	cubic-Pn3m d_{100}	cubic-Im3m d_{100}	H_{II} d_{10}	
2-11.1.4	11	1 M	1,6 Hexanediol		0.01 M	Co chloride	0.1 M	Na acetate	4.6		49.4						
2-33.1.4	33	2 M	Ammonium formate				0.1 M	HEPES	7.5		49.4						
2-31.1.4	31	20%	Jeffamine M-600				0.1 M	HEPES	7.5		49.5						**
2-29.1.4	29	30%	MPD		0.5 M	Ammonium sulfate	0.1 M	HEPES	7.5			40.9					
2-13.1.4	13	30%	PEG MME 2000		0.2 M	Ammonium sulfate	0.1 M	Na acetate	4.6			46.3		(95)			†, ‖
2-26.1.4	26	30%	PEG MME 5000		0.2 M	Ammonium sulfate	0.1 M	MES	6.5			46.6					†
2-7.1.4	7	10% 10%	PEG 1000 PEG 8000									47.3					
2-38.1.4	38	20%	PEG 10,000				0.1 M	HEPES	7.5			48					
2-30.1.4	30	10% 5%	PEG 6000 MPD				0.1 M	HEPES	7.5			48.4	167				
2-22.1.4	22	12%	PEG 20,000				0.1 M	MES	6.5			48.9					
2-24.1.4	24	30%	Jeffamine M-600		0.05 M	Cs chloride	0.1 M	MES	6.5			49.2	206	133			†, ‡, §
2-46.1.4	46	30%	PEG MME 550		0.1 M	Na chloride	0.1 M	Bicine	9			49.2					
2-3.1.4	3	25%	Ethylene glycol									49.4					††
2-35.1.4	35	70%	MPD				0.1 M	HEPES	7.5			49.5					
2-10.1.4	10	30%	MPD		0.2 M	Na chloride	0.1 M	Na acetate	4.6			49.7					
2-4.1.4	4	35%	Dioxane									49.8					**
2-19.1.4	19	2.5 M	1,6 Hexanediol				0.1 M	Na citrate	5.6			50.5					
2-43.1.4	43	50%	MPD		0.2 M	Ammonium phosphate	0.1 M	Tris	8.5			58					¶
2-39.1.4	39	3.4 M	1,6 Hexanediol		0.2 M	Mg chloride	0.1 M	Tris	8.5			64.5					¶
2-1.1.4	1	10%	PEG 6000		2 M	Na chloride							160				
2-37.1.4	37	10% 8%	PEG 8000 Ethylene glycol				0.1 M	HEPES	7.5				164				
2-41.1.4	41	1M	Li sulfate		0.01 M	Ni chloride	0.1 M	Tris	8.5					89			
2-42.1.4	42	12%	Glycerol		1.5 M	Ammonium sulfate	0.1 M	Tris	8.5					92			
2-48.1.4	48	10%	PEG 20,000		2%	Dioxane	0.1 M	Bicine	9					97			
2-28.1.4	28	1.6 M	Sodium citrate	6.5										99			†
2-14.1.4	14	2 M	Ammonium sulfate		0.2 M	K, Na tartrate	0.1 M	Na citrate	5.6					103			
2-32.1.4	32	1.6 M	Ammonium sulfate		0.1 M	Na chloride	0.1 M	HEPES	7.5					104			
2-36.1.4	36	4.3 M	Na chloride				0.1 M	HEPES	7.5					104			
2-47.1.4	47	2 M	Mg chloride				0.1 M	Bicine	9					108			
2-25.1.4	25	1.8 M	Ammonium sulfate		0.01 M	Co chloride	0.1 M	MES	6.5					109			
2-15.1.4	15	1M	Li sulfate		0.5 M	Ammonium sulfate	0.1 M	Na citrate	5.6					109			
2-5.1.4	5	5%	Isopropanol		2 M	Ammonium sulfate								110			
2-18.1.4	18	10%	Jeffamine M-600		0.01 M	Fe chloride	0.1 M	Na citrate	5.6					112			
2-20.1.4	20	1.6 M	Mg sulfate				0.1 M	MES	6.5					113			
2-23.1.4	23	10%	Dioxane		1.6 M	Ammonium sulfate	0.1 M	MES	6.5					114			
2-34.1.4	34	1 M	Na acetate		0.05 M	Cd sulfate	0.1 M	HEPES	7.5					114			
2-27.1.4	27	25%	PEG MME 550		0.01 M	Zn sulfate	0.1 M	MES	6.5					116			†
2-13.1.4	12	30%	PEG 400		0.1 M	Cd chloride	0.1 M	Na acetate	4.6					116			
2-2.1.4	2	0.01 M 0.5 M	Mg chloride Na chloride		0.01 M	CTAB								116			
2-6.1.4	6	1 M	Imidazole	7										116			
2-9.1.4	9	2 M	Na chloride				0.1 M	Na acetate	4.6					118			
2-21.1.4	21	2 M	Na chloride		0.2 M	Na, K phosphate	0.1 M	MES	6.5					118			
0.1.4	**0**													**119**			**†**
2-8.1.4	8	10%	Ethanol		1.5 M	Na chloride								119			
2-17.1.4	17	35%	tert-Butanol				0.1 M	Na citrate	5.6					129			
2-16.1.4	16	4%	Polyethyleneimine		0.5 M	Na chloride	0.1 M	Na citrate	5.6					131			
2-45.1.4	45	20%	PEG MME 2000		0.01 M	Ni chloride	0.1 M	Tris	8.5						126		
2-44.1.4	44	20%	Ethanol				0.1 M	Tris	8.5		(49.4)				147		†, ‖
2-40.1.4	40	25%	tert-Butanol		0.1 M	Ca chloride	0.1 M	Tris	8.5						152		

TABLE 1.—*Continued*

Screen 1, Prep. 2, 4 °C

Code	Crystal screen solution no.	Screen composition*							Phase identification and structure parameter (Å)							Footnotes
		Precipitant		Salt		Buffer										
		Concen-tration	Identity	Concen-tration	Identity	Concen-tration	Identity	pH	FI	L_c d_{001}	L_α d_{001}	cubic-Ia3d d_{100}	cubic-Pn3m d_{100}	cubic-Im3m d_{100}	H_{II} d_{10}	
1-14.2.4	14	28%	PEG 400	0.2 M	Ca chloride	0.1 M	HEPES	7.5		49.4						**
1-16.2.4	16	1.5 M	Li sulfate			0.1 M	HEPES	7.5		49.4						**
1-2.2.4	2	0.4 M	K, Na tartrate							49.5						
1-8.2.4	8	30%	Isopropanol	0.2 M	Na citrate	0.1 M	Na cacodylate	6.5		49.5						
1-10.2.4	10	30%	PEG 4000	0.2 M	Ammonium acetate	0.1 M	Na acetate	4.6		49.5						**
1-18.2.4	18	20%	PEG 8000	0.2 M	Mg acetate	0.1 M	Na cacodylate	6.5		49.5						
1-13.2.4	31	30%	PEG 4000	0.2 M	Ammonium sulfate					49.5						
1-47.2.4	47	2 M	Ammonium sulfate			0.1 M	Na acetate	4.6		49.5						
1-37.2.4	37	8%	PEG 4000			0.1 M	Na acetate	4.6		49.5						
1-32.2.4	32	2 M	Ammonium sulfate							49.5						†, **
1-48.2.4	48	2 M	Ammonium phosphate			0.1 M	Tris	8.5		49.5						†
1-40.2.4	40	20% 20%	Isopropanol PEG 4000			0.1 M	Na citrate	5.6			40.8					
1-41.2.4	41	10% 20%	Isopropanol PEG 4000			0.1 M	HEPES	7.5			42.7					†
1-43.2.4	43	30%	PEG 1500								43.5					
1-13.2.4	13	30%	PEG 400	0.2 M	Na citrate	0.1 M	Tris	8.5			44					
1-9.2.4	9	30%	PEG 4000	0.2 M	Ammonium acetate	0.1 M	Na citrate	5.6			44.1					
1-15.2.4	15	30%	PEG 8000	0.2 M	Ammonium sulfate	0.1 M	Na cacodylate	6.5			44.2					†
1-5.2.4	5	30%	MPD	0.2 M	Na citrate	0.1 M	HEPES	7.5			44.3					
1-34.2.4	34	2 M	Na formate			0.1 M	Na acetate	4.6			44.3					
1-20.2.4	20	25%	PEG 4000	0.2 M	Ammonium sulfate	0.1 M	Na acetate	4.6			44.9					
1-42.2.4	42	20%	PEG 8000	0.05 M	K phosphate						45.1					†
1-45.2.4	45	18%	PEG 8000	0.2 M	Zn acetate	0.1 M	Na cacodylate	6.5			45.2					†
1-33.2.4	33	4 M	Na formate								45.3	158				
1-30.2.4	30	30%	PEG 8000	0.2 M	Ammonium sulfate						45.3					
1-17.2.4	17	30%	PEG 4000	0.2 M	Li sulfate	0.1 M	Tris	8.5			45.7	(111)				‖
1-46.2.4	46	18%	PEG 8000	0.2 M	Ca acetate	0.1 M	Na cacodylate	6.5			45.8					
1-12.2.4	12	30%	Isopropanol	0.2 M	Mg chloride	0.1 M	HEPES	7.5			47.3					
1-28.2.4	28	30%	PEG 8000	0.2 M	Na acetate	0.1 M	Na cacodylate	6.5			47.6					
1-19.2.4	19	30%	Isopropanol	0.2 M	Ammonium acetate	0.1 M	Tris	8.5			47.8					
1-26.2.4	26	30%	MPD	0.2 M	Ammonium acetate	0.1 M	Na citrate	5.6			48.1					
1-21.2.4	21	30%	MPD	0.2 M	Mg acetate	0.1 M	Na cacodylate	6.5			48.4					
1-1.2.4	1	30%	MPD	0.02 M	Ca chloride	0.1 M	Na acetate	4.6			50.9					
1-27.2.4	27	20%	Isopropanol	0.2 M	Na citrate	0.1 M	HEPES	7.5			52.1					
1-24.2.4	24	20%	Isopropanol	0.2 M	Ca chloride	0.1 M	Na acetate	4.6			54					
1-22.2.4	22	30%	PEG 4000	0.2 M	Na acetate	0.1 M	Tris	8.5				106				‡, **
1-6.2.4	6	30%	PEG 4000	0.2 M	Mg chloride	0.1 M	Tris	8.5				107				‡
1-36.2.4	36	8%	PEG 8000			0.1 M	Tris	8.5				122				
1-50.2.4	50	15%	PEG 8000	0.5 M	Li sulfate							132				
1-7.2.4	7	1.4 M	Na acetate			0.1 M	Na cacodylate	6.5				161				
1-44.2.4	44	0.2 M	Mg formate									164				
1-11.2.4	11	1 M	Ammonium phosphate			0.1 M	Na citrate	5.6				169				
1-39.2.4	39	2% 2 M	PEG 400 Ammonium sulfate			0.1 M	HEPES	7.5				170				
1-3.2.4	3	0.4 M	Ammonium phosphate									172				
0.2.4	**0**									**(49.5)**		**173**				**†, ‖**
1-49.2.4	49	2%	PEG 8000	1 M	Li sulfate								94			
1-35.2.4	35	1.6 M	Na, K phosphate			0.1 M	HEPES	7.5					101			
1-29.2.4	29	0.8 M	K, Na tartrate			0.1 M	HEPES	7.5					104			†, ‡
1-25.2.4	25	1 M	Na acetate			0.1 M	Imidazole	6.5					109			
1-23.2.4	23	30%	PEG 400	0.2 M	Mg chloride	0.1 M	HEPES	7.5					110			
1-4.2.4	4	2 M	Ammonium sulfate			0.1 M	Tris	8.5							50.6	
1-38.2.4	38	1.4 M	Na citrate			0.1 M	HEPES	7.5							52	

TABLE 1.—*Continued*

Screen 2, Prep. 2, 4 °C

Code	Crystal screen solution no.	Screen composition*								Phase identification and structure parameter (Å)							Footnotes
		Precipitant			Salt		Buffer										
		Concentration	Identity	pH	Concentration	Identity	Concentration	Identity	pH	FI	L_c d_{001}	L_α d_{001}	cubic-Ia3d d_{100}	cubic-Pn3m d_{100}	cubic-Im3m d_{100}	H_{II} d_{10}	
2-35.2.4	35	70%	MPD				0.1 M	HEPES	7.5	34.8	(49.4)						†, ‖
2-5.2.4	5	5%	Isopropanol		2 M	Ammonium sulfate					49.4	38.5					
2-20.2.4	20	1.6 M	Mg sulfate				0.1 M	MES	6.5		49.4						†
2-36.2.4	36	4.3 M	Na chloride				0.1 M	HEPES	7.5		49.4						**
2-48.2.4	48	10%	PEG 20,000		2%	Dioxane	0.1 M	Bicine	9		49.4						†, **
2-46.2.4	46	30%	PEG MME 550		0.1 M	Na chloride	0.1 M	Bicine	9		49.4						**
2-44.2.4	44	20%	Ethanol				0.1 M	Tris	8.5		49.5	39.1					
2-29.2.4	29	30%	MPD		0.5 M	Ammonium sulfate	0.1 M	HEPES	7.5		49.5						
2-28.2.4	28	1.6 M	Na citrate	6.5							49.5						**
2-31.2.4	31	20%	Jeffamine M-600				0.1 M	HEPES	7.5		49.5						†
2-43.2.4	43	50%	MPD		0.2 M	Ammonium phosphate	0.1 M	Tris	8.5			41.2					
2-26.2.4	26	30%	PEG MME 5000		0.2 M	Ammonium sulfate	0.1 M	MES	6.5			44.4					†
2-7.2.4	7	10% 10%	PEG 1000 PEG 8000									44.7					
2-13.2.4	13	30%	PEG MME 2000		0.2 M	Ammonium sulfate	0.1 M	Na acetate	4.6			44.7					†
2-38.2.4	38	20%	PEG 10,000				0.1 M	HEPES	7.5			44.8					
2-4.2.4	4	35%	Dioxane									44.9					
2-45.2.4	45	20%	PEG MME 2000		0.01 M	Ni chloride	0.1 M	Tris	8.5			45					†
2-30.2.4	30	10% 5%	PEG 6000 MPD				0.1 M	HEPES	7.5			46					
2-37.2.4	37	10% 8%	PEG 8000 Ethylene glycol				0.1 M	HEPES	7.5			46.3					
2-22.2.4	22	12%	PEG 20,000				0.1 M	MES	6.5			46.3					
2-2.2.4	2	0.01 M 0.5 M	Mg chloride Na chloride		0.01 M	CTAB						46.8					
2-17.2.4	17	35%	tert-Butanol				0.1 M	Na citrate	5.6			46.8					
2-40.2.4	40	25%	tert-Butanol		0.1 M	Ca chloride	0.1 M	Tris	8.5			46.9					
2-10.2.4	10	30%	MPD		0.2 M	Na chloride	0.1 M	Na acetate	4.6			48.6					
2-39.2.4	39	3.4 M	1,6 Hexanediol		0.2 M	Mg chloride	0.1 M	Tris	8.5			48.9					
2-6.2.4.	6	1 M	Imidazole	7								49.1	166				
2-8.2.4	8	10%	Ethanol		1.5 M	Na chloride						49.2	168				
2-3.2.4	3	25%	Ethylene glycol									49.4					††
2-27.2.4	27	25%	PEG MME 550		0.01 M	Zn sulfate	0.1 M	MES	6.5			49.4					††
2-11.2.4	11	1 M	1,6 Hexanediol		0.01 M	Co chloride	0.1 M	Na acetate	4.6			50.5					
2-18.2.4	18	10%	Jeffamine M-600		0.01 M	Fe chloride	0.1 M	Na citrate	5.6			50.8	190				
2-24.2.4	24	30%	Jeffamine M-600		0.05 M	Cs chloride	0.1 M	MES	6.5			51.7					
2-19.2.4	19	2.5 M	1,6 Hexanediol				0.1 M	Na citrate	5.6			53.2					
2-1.2.4	1	10%	PEG 6000		2 M	Na chloride							138				
2-16.2.4	16	4%	Polyethyleneimine		0.5 M	Na chloride	0.1 M	Na citrate	5.6				158				
2-9.2.4	9	2 M	Na chloride				0.1 M	Na acetate	4.6				159				
0.2.4	**0**										**(49.5)**		**173**				**†, ‖**
2-15.2.4	15	1M	Li sulfate		0.5 M	Ammonium sulfate	0.1 M	Na citrate	5.6					84			
2-14.2.4	14	2 M	Ammonium sulfate		0.2 M	K, Na tartrate	0.1 M	Na citrate	5.6					85			
2-41.2.4	41	1M	Li sulfate		0.01 M	Ni chloride	0.1 M	Tris	8.5					87		54.2	
2-23.2.4	23	10%	Dioxane		1.6 M	Ammonium sulfate	0.1 M	MES	6.5					89			‡
2-32.2.4	32	1.6 M	Ammonium sulfate		0.1 M	Na chloride	0.1 M	HEPES	7.5					90			
2-25.2.4	25	1.8 M	Ammonium sulfate		0.01 M	Co chloride	0.1 M	MES	6.5					93			
2-47.2.4	47	2 M	Mg chloride				0.1 M	Bicine	9					102			†
2-34.2.4	34	1 M	Na acetate		0.05 M	Cd sulfate	0.1 M	HEPES	7.5					103			
2-33.2.4	33	2 M	Ammonium formate				0.1 M	HEPES	7.5					107			
2-12.2.4	12	30%	PEG 400		0.1 M	Cd chloride	0.1 M	Na acetate	4.6		(49.5)			108			†, ‖
2-21.2.4	21	2 M	Na chloride		0.2 M	Na, K phosphate	0.1 M	MES	6.5					109			
2-42.2.4	42	12%	Glycerol		1.5 M	Ammonium sulfate	0.1 M	Tris	8.5							53.7	

TABLE FOOTNOTES

Hampton Screen (Screen 1) and Hampton Screen 2 (Screen 2) solutions were used according to the following recipes: Prep. 1, monoolein/screen solution/water (3:2:2 by wt.); Prep. 2, monoolein/screen solution (3:2 by wt.).

*Classification of screen components as precipitant, salt or buffer as specified by supplier.

†Structure parameters represent the average of at least duplicate measurements. Repeated sample preparation followed by diffraction measurements show that the structure parameter errors are as follows: 0.5–1 Å, FI; 0.1–0.2 Å, L_c; 0.5–2 Å, L_α; 2–3 Å, cubics; 5–10 Å, for disordered cubics with large structure parameters (e.g., 1-26.1.20, 2-24.1.20), and 0.5–1 Å, H_{II}.

‡Spotty diffraction pattern. The cubic phases are particularly prone to growing large crystallites, which give rise to spotty patterns (Fig. 4 *G*).

§Disordered cubic phase, possibly a sponge phase (Fig. 4 *I*).

‖Most samples produced a single phase with a single structure parameter. Some however, form coexisting phases. These are indicated by two, and possibly three, structure parameters for a given sample or screen solution number. Round brackets are used to indicate that different phase behavior was observed with replicate samples. Thus, for example, 1-19.1.4 produced the cubic-Ia3d phase in one replicate (no brackets), the cubic-Pn3m phase in a second replicate (one bracket), and the L_α phase in a third replicate (two brackets).

¶Substantial amount of diffuse scatter in the diffraction pattern accompanies the identified phase (Fig. 4 *H*).

#No diffraction observed. Sample is possibly a liquid under these conditions.

**Small amount of an unidentified phase coexists with the reported phase.

††Lamellar phase type is uncertain because wide-angle diffraction/scattering intensity is low. Could be L_c or L_α phase.

structure parameter values are reported for a given sample. Replicate samples that produced different phases are identified by structure parameter values in round brackets (Table 1, footnote ‖).

To facilitate discussion, entries in Table 1 have been assigned an identity code based on Screen number (1; 2), Screen solution number (1 to 50 for Screen 1; 1 to 48 for Screen 2), sample preparation protocol type (Prep. 1; Prep. 2) and temperature (4°C; 20°C), in that order. Thus, the identifier "2–35.1.4" refers to a sample prepared using solution 35 from Screen 2 with the Prep. 1 protocol at 4°C.

Table 1 encompasses several variables and, of necessity, is quite large. To get a sense of the number of screen solutions that are cubic phase compatible, one needs only to peruse the cubic phase columns under Phase Identification in the table and locate those entries with cubic phase lattice parameter values.

No attempt will be made to describe every screen solution and its compatibility, or otherwise, with the *in meso* method under the assorted conditions examined. However, there are some general trends that are worthy of note. Further, the data make sense in the context of the generalized phase behavior of the monoolein/water system (Fig. 2) as will be discussed.

The results of measurements performed at 20°C will be considered first. Here, all but two of the Screen 1 series produced the cubic phase when samples were prepared using the Prep. 1 protocol, where an excess of aqueous phase is present. The same general result was obtained with the Screen 2 series under these same conditions, although one of the solutions did give rise to problems with data analysis (2–35.1.20). When the measurements were repeated using the Prep. 2 protocol, which produces samples that are stressed with regard to aqueous medium, a dramatic drop in the number of Screen 1 and Screen 2 solutions capable of supporting the cubic phase was observed. Here, only 50% of either screen type went on to produce the cubic phase. The non-cubic phases encountered under these conditions were predominantly of the L_α and H_{II} type.

In contrast to the data at 20°C, those at 4°C show that the yield of cubic phase fell and that the frequency of occurrence of the L_c and L_α phases rose. Following the Prep. 1 protocol, between 50% and 60% of the Screen 1 and Screen 2 solutions gave rise to the cubic phase. The H_{II} phase was not seen under these conditions. With Prep. 2, the cubic phase was observed only 25% of the time with Screen 1 and Screen 2. The L_c phase figured prominently as a non-cubic phase under these conditions. These data recorded at 4 and 20°C are summarized in the form of histograms in Fig. 5.

The reference samples used in this study are identified in Table 1 as Screen Solution 0. They correspond to monoolein dispersed in water alone at 40 and 57% (w/w) water. At 20°C, the cubic-Pn3m phase was observed for both (entries 0.2.20 and 0.1.20, respectively) as expected (Points IV and V, respectively in Fig. 2 *A*). The respective lattice parameter values of 102 Å and 107 Å are consistent with the different levels of hydration in each. At 4°C on the other hand, intermittent phase behavior was observed (entries 0.2.4 and 0.1.4) as was expected under these so-called metastable conditions (Qiu and Caffrey, 2000). Metastability is examined in more detail below.

DISCUSSION

Interpreting the results

The original *in meso* method was developed with reference to the lyotropic (water-dependent) and thermotropic (temperature-dependent) phase behavior of the monoolein/water system (Fig. 2), and was implemented at 20°C. We interpret the effect on mesophase stability of screen components, preparation protocol, and temperature by referring also to the phase diagram of the monoolein/water system (Fig. 2). It is important to note that the latter represents a simple two-component system consisting of lipid and water only. In what follows, we will take the liberty of sometimes disregarding the components of a given screen and simply view the solution as a means for hydrating the lipid. At other times, the focus will be on the screen components as we seek to make sense of the changes they trigger in mesophase type and phase microstructure. In reading Fig. 2, it should be noted that phase boundary locations are approximate.

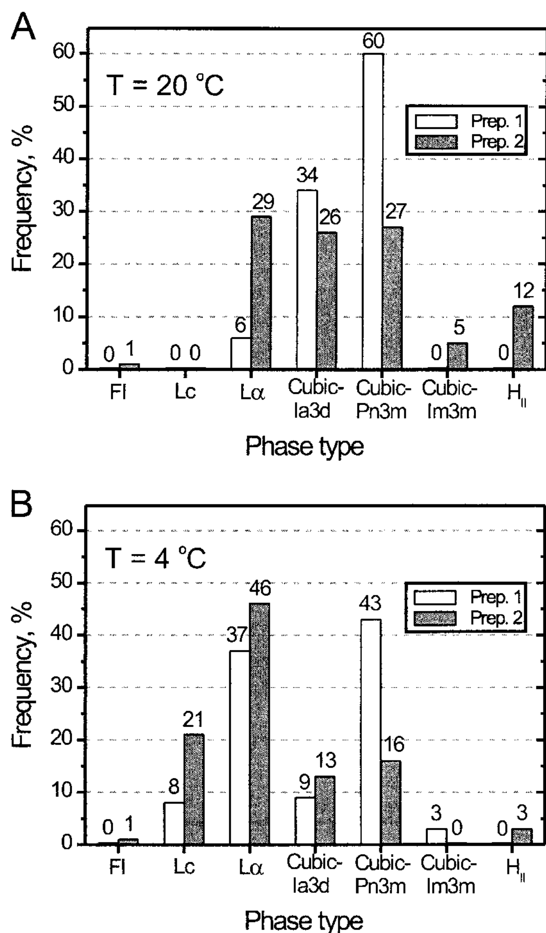

FIGURE 5 Frequency with which the different phases form when monoolein is combined with the Hampton screen solutions under Prep. 1 and Prep. 2 protocols at 20°C (*A*) and at 4°C (*B*). Phase determination was made after incubation times of at least 1 day at 20°C and 3 to 4 weeks at 4°C. Frequency is expressed as a percentage, where 100% represents 98 test solutions from the Hampton Screen (50 solutions) and Screen 2 (48 solutions) series.

The estimated error in composition and temperature are 3% (w/w) water and 3°C, respectively (Qiu and Caffrey, 2000).

Before proceeding to interpret the results in Table 1, it is instructive to examine briefly the phase behavior of the monoolein/water system along the relevant 20°C isotherm in Fig. 2. The dry lipid at 20°C exists in the solid state represented by the L_c phase (Point I in Fig. 2 *A*). Upon hydration, the L_c phase transforms sequentially through the L_α (Point II in Fig. 2 *A*) and cubic-Ia3d phases (Point III in Fig. 2A) to the cubic-Pn3m phase (Point IV in Fig. 2 *A*). Further addition of water, beyond the saturation limit of the cubic-Pn3m phase, results in coexistence of the fully hydrated cubic-Pn3m phase and bulk water (Point V in Fig. 2 *A*). Two sample preparation protocols were used in the current study. One (Prep. 1) used a monoolein/aqueous solution mixture in the weight ratio 43:57. This corresponds to Point V in Fig. 2 *A* and to the fully hydrated condition if the screen solution consisted only of water. In contrast, Prep. 2 contained 40% (w/w) aqueous solution corresponding to Point IV in Fig. 2 *A*. Under this condition, the system should be water-stressed, i.e., have no excess water, and produce the cubic-Pn3m phase when water, as opposed to a screen solution, is the lyotrope or dispersing medium.

Attempting to ascribe an effect on phase behavior and phase microstructure to a given screen constituent is complicated by the variety of components, and their respective concentrations, present in each screen solution. Accordingly, systematic comparisons are difficult in the absence of a complete statistical study. Of course, this does not impact on the survey aspect of the work. Ultimately, however, we seek an understanding of the effects of individual components and how they operate in concert. In what follows, we will identify only those factors having a major influence on phase properties and microstructure. Given that the hosting lipid, monoolein, does not engage in protonic equilibrium, its uncharged state should not change in the pH range covered (buffer pH: 4.6–8.5).

Prep. 1 conditions at 20°C

With a view to facilitating an analysis of the effects of the different screens and their components on monoolein mesophase and phase microstructure, selected data from Table 1 are presented graphically in Fig. 6. When examining these plots it is important to bear in mind that the measurements upon which they are based were made in multicomponent systems, and that the lattice parameter in the different phases is presented as a function of the concentration of just one of these components. In the case of Fig. 6 *A*, the component in question is a salt. The higher molecular weight polyethylene glycols (PEGs) are represented in Fig. 6 *B*, and the smaller organics, mostly alcohols, are included in Fig. 6 *C*. Presenting the data in this way allows for trends to be identified more easily. In what follows, the effects of the assorted screen components are examined in more detail.

Referring to the Screen 1 data (Table 1) we find that the following components do not perturb the identity of the cubic phase under Prep. 1 conditions: iso-propanol, a variety of salts and buffers, the low molecular weight PEGs, and the higher molecular weight PEGs at low concentrations. An effect is seen, however, on the lattice parameter of the cubic-Pn3m phase. Specifically, iso-propanol consistently caused the cubic-Pn3m phase to swell, as evidenced by an elevated lattice parameter. In contrast, high salt concentration lowered the lattice parameter of the cubic-Pn3m phase (Fig. 6 *A*). The relative lattice contraction strength of the different salt anions is as follows: citrate $\approx$ sulfate $>$ tartrate $>$ phosphate $>$ formate $>$ acetate $>$ chloride. Thus, citrate and sulfate had the largest effect on cubic-Pn3m lattice-size, whereas the effect of chloride ions was minor at the same concentration. Because the hosting lipid, monoo-

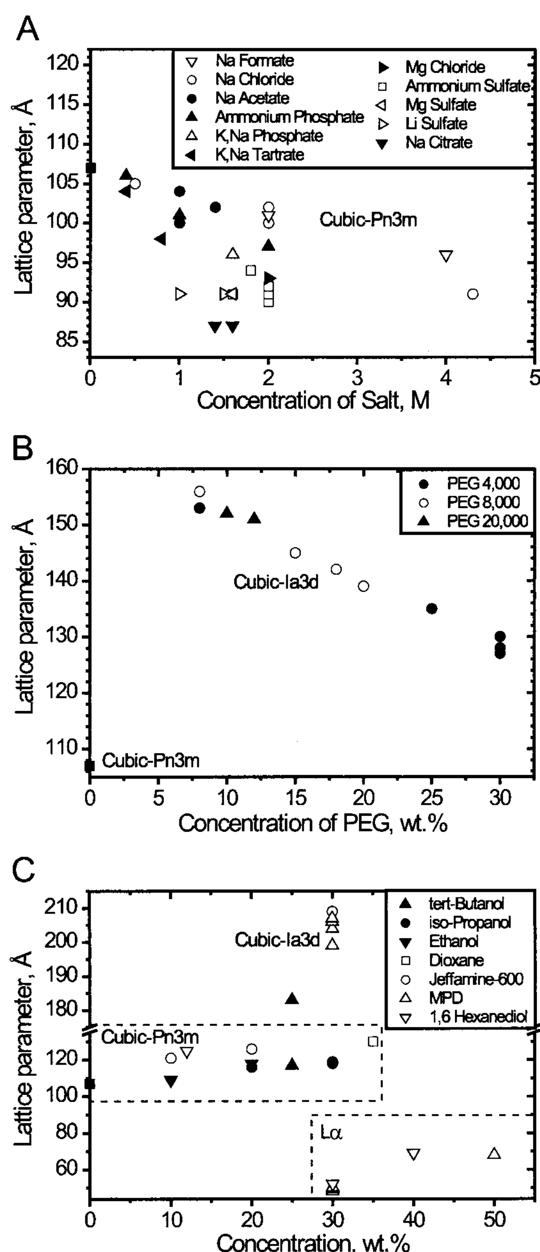

FIGURE 6 Dependence of the phase lattice parameter on the concentration of a particular screen component when Hampton screen solutions were dispersed and incubated with monoolein at 20°C after the Prep. 1 protocol. The different components include salts (*A*), high molecular weight PEGs (*B*), and an assortment of relatively small organics, mostly alcohols (*C*). The phase associated with a given set of data is indicated.

lein, is uncharged and does not engage in protonic equilibrium, charge screening or direct electrostatic interaction are unlikely to account for these effects. However, the hydroxyls and ester linkage on the lipid headgroup may coordinate with the ions in an ion-specific way so as to alter the effective size of the lipid polar moiety relative to that of the long apolar chain. This in turn would change the curvature at the apolar/polar interface, giving rise to a smaller lattice parameter as curvature is increased.

The higher molecular weight PEGs brought about a shift from the cubic-Pn3m to the cubic-Ia3d phase and a unit cell contraction with increasing polymer concentration (Fig. 6 *B*). This is consistent with the water-withdrawing effect of large PEG molecules which, because of their size, are excluded from the aqueous matrix of the cubic medium. The dialcohol, 2-methyl-2,4-pentanediol (MPD), produced disordered cubic phases with large lattice parameters. MPD as well as iso-propanol when used at high concentration or in combination with PEG destabilized the cubic phase in favor of the lamellar phase (Fig. 6 *C*). In the context of the monoolein/water phase diagram (Fig. 2 *A*), these observations are consistent with a rather severe osmotic effect possibly coupled with an effect of the dialcohol on bilayer curvature.

With one notable exception, the same general trends were observed for the Screen 2 solutions under Prep. 1 conditions as noted above for Screen 1. The exception was a sample prepared with a screen solution containing 70% MPD that gave no measurable diffraction (2–35.1.20). The result is not unexpected given the extraordinarily high organic solvent content of the solution. It is likely that the dialcohol simply dissolved the hydrated lipid.

Prep. 2 conditions at 20°C

Prep. 2 conditions brought about a substantial change in phase behavior when compared to that observed following the Prep. 1 protocol (Fig. 5 *A*). This was expected given that the samples now contain a maximum of 40% (w/w) aqueous medium which corresponds to the water-stressed condition (Point IV in Fig. 2 *A*). Thus, any screen component that has an osmotic effect should immediately shift phase behavior in the direction of less hydration, i.e., to the left along the 20°C isotherm in Fig. 2 *A*. This is exactly what we see for both Screens 1 and 2 where all but one solution gave rise to a cubic-Pn3m phase with a lattice parameter less than that of the reference (0.2.20). Under Prep. 2 conditions, iso-propanol stabilized the L_α phase, presumably by being forced into the bilayer and/or sufficiently modifying the dielectric properties of the confined aqueous channels within the mesophase. The larger PEGs again stabilized the cubic-Ia3d and/or the L_α phases consistent with their osmotic properties. MPD and iso-propanol/PEG had the same effect as seen under Prep. 1 conditions. Here, however, the 2–35 screen solution containing 70% MPD produced a fully developed and easily recognizable FI phase (2–35.2.20; Fig. 1). This presumably reflects the higher overall concentration of lipid and other components in the sample. Another notable feature of the Prep. 2 conditions was the emergence of the H_{II} phase. In the monoolein/water phase diagram (Fig. 2), the pure H_{II} phase comes in at relatively low hydration levels and high temperatures. Separate studies show that high salt concentrations stabilize the H_{II} phase in hydrated monoolein at close to room temperature (Caffrey, 1987). Consistent with this is the finding that high salt,

particularly of the sulfate type, in the screen solutions is precisely what gives rise to the H_{II} phase. The Prep. 2 conditions also facilitated accessing one of the less common isotropic mesophases, the cubic-Im3m phase. Elevated concentrations of Jeffamine and high molecular weight polyethylene glycol monomethyl ether favored the latter as did the bigger PEGs. The cubic-Im3m phase has been observed previously in the monoolein/water system, but the conditions that stabilize it have not been established (Caffrey, 1987).

By way of summarizing cubic phase compatibility at 20°C, we note that ~90% of the solutions in the Screen 1 and Screen 2 series gave rise to one or other of the cubic mesophases under Prep. 1 conditions. This figure dropped to a little over 50% when Prep. 2 conditions were imposed (Fig. 5 *A*).

Measurements at 4°C

The corresponding percentages at 4°C were 50 to 60% for Prep. 1 and 25% for Prep. 2 (Fig. 5 *B*). The data collected at this low temperature represent a special and somewhat more complicated case where undercooling (also referred to as metastability) prevails (Qiu and Caffrey, 2000). This important and practical issue is discussed in more detail below.

Undercooling and metastability

Crystallization trials are usually carried out at several temperatures (McPherson, 1999). Likewise, it will be desirable to implement the *in meso* method at temperatures both above, but more frequently, below 20°C, the temperature at which the method was developed. The current study incorporated such an evaluation of temperature effects, with measurements conducted at 4°C and at 20°C.

The importance of temperature in the current study should be apparent in light of the thermal sensitivity of the hosting cubic phase (Briggs et al., 1996; Qiu and Caffrey, 2000). With reference to the equilibrium monoolein/water phase diagram in Fig. 2 *B*, we see that the standard procedure for preparing *in meso* crystallization samples containing 60% (w/w) lipid and 40% (w/w) aqueous medium gives rise to the cubic phase at 20°C. However, when temperature is dropped to 4°C, the L_c phase replaces the cubic phase (Fig. 2 *B*). The L_c phase represents the solid state. It is not a liquid crystal and accordingly is unlikely to support protein reconstitution and crystal growth. Thus, it is to be avoided. With this as background and considering the data in Table 1, the obvious question arises as to how the cubic as well as other liquid crystal phases were accessed and the undesirable L_c phase avoided in many of the trials conducted at 4°C. The answer lies in our ability to exploit the natural inclination of lipidic liquid crystal phases to undercool in the same way that water, cooled appropriately, remains liquid to temperatures well below 0°C. Thus, the experimental protocol for making measurements at 4°C involved an initial mixing of lipid and screen solution at 20°C, followed by cooling. This procedure allows the cubic phase to undercool and to persist in a metastable state at 4°C. Under equilibrium conditions, it would have reverted to the more thermodynamically stable L_c phase.

The cubic phase is notorious in its capacity to undercool, a state in which it can remain for years. Indeed, biological significance has been attached to this property of the cubics (Luzzati, 1997). However, despite the ability to access the undercooled cubic phase and thus, to use it in *in meso* crystallization trials at 4°C, one must remain mindful of the fact that such a system is intrinsically unstable. It can revert at any time to another equilibrium phase, which may not be compatible with growing protein crystals.

The data in Table 1 lend credence to the above statements. Thus, for example, the L_c phase was not observed in any of the trials regardless of preparation protocol when samples were processed entirely at 20°C. In distinct contrast, trials performed at 4°C produced the L_c phase in close to 1 in every 5 samples. Further, the L_c phase figured prominently when intermittent phase behavior was observed (bracketed lattice parameters in Table 1). This is a hallmark of metastability. As noted, it revealed itself also in the case of the reference sample (0.2.4 in Table 1).

Choice of screen concentration

Before proceeding with a further consideration of the results, the reasons for choosing the particular lipid-to-screen solution ratios used in the study will be given. As noted, two types of sample preparations were used. One was inspired by the original *in meso* method protocol where the cubic phase was prepared at 20°C by combining 60% (w/w) monoolein with 40% (w/w) aqueous medium. Under these conditions, the cubic phase, presumably at less than full hydration (Point IV in Fig. 2 *A*), was accessed. In the current study, we simply replaced the aqueous medium referred to above with undiluted screen solution. This is what we refer to as Prep. 2. In related studies, the soluble proteins, lysozyme and thaumatin, have been crystallized *in meso* using this recipe. To this end, each protein was dissolved in an appropriate aqueous solution which was then used to form the cubic phase from which crystals grew (Caffrey, 2000).

The second sample preparation protocol, Prep. 1, is a variation of Prep. 2 in that the same ratio (3:2 by weight) of monoolein-to-undiluted screen solution was used. However, in this case we followed the supplier's recommendation of using half-strength screen. The sample consisted of monoolein, undiluted screen, and water in the ratio 3:2:2 by weight. The final sample consisted of 57% (w/w) aqueous phase and 43% (w/w) monoolein. If the aqueous medium was replaced entirely by water, such a mix at 20°C would

produce the cubic-Pn3m phase in equilibrium with bulk water (Point V in Fig. 2 *A*).

While this explains the reality of the situation, Prep. 1 was in fact inspired by a scenario in which the cubic phase is formed in a standard crystallization trial with 60% (w/w) monoolein and 40% (w/w) protein-containing aqueous solution. A quantity of undiluted screen solution, equal in volume to that present in the cubic phase sample, is subsequently layered on top of the preformed cubic phase and allowed to equilibrate with it. Assuming that all screen components can diffuse into the aqueous compartments of the cubic phase, the original screen solution would be diluted by half upon establishing equilibrium. This is the condition we wished to simulate by using a 1:1 dilution of the screen solution in Prep. 1.

Relevance of the experimental protocol

The current study was performed starting with homogenous mixtures of lipid and screen solution. One obvious question regarding this approach concerns its relevance to the manner in which actual crystallization trials are performed. In our lab, several *in meso* crystallization protocols are used that include the approaches implemented in the current study. In this regard, the work and the results are relevant. Another approach being used involves dispersing the lipid with the aqueous protein solution in the proper mass ratio and at the right temperature so as to produce the cubic phase spontaneously in the absence of precipitants. The screen solution is then layered on top of the preformed cubic phase and the two allowed to equilibrate. During the equilibration process, transient gradients form throughout the cubic phase. These consist of the low molecular weight, diffusable components of the screen solution. The larger polymeric materials would effectively be excluded from the mesophase altogether. The rate at which the diffusables move into the cubic phase depends, among other things, on molecular size and shape, and on solubility in the aqueous and apolar lipidic portions of the cubic medium (Gerritsen and Caffrey, 1990). The lifetime and the profile of the gradients likewise depend on many variables. During the course of what is likely to be an extremely complex equilibration process, the cubic phase will encounter vast changes in its local chemical environment. These may be extreme enough to destroy the cubic phase completely. By the same token, the conditions may alter the cubic phase or perhaps induce the formation of an adjacent coexisting phase in a way that promotes protein crystal nucleation and growth (Caffrey, 2000). Such changes are likely to be local, and though they may prove to be important in terms of growing crystals, we did not attempt to monitor them in the current study. To do so would require special sample holding devices and focused, micrometer-sized x-ray beams.

Cubic phase identity

In this study, we have identified the phases formed by monoolein in combination with screen solutions under specified conditions by means of low- and wide-angle x-ray diffraction. Our primary interest is in the cubic phase since this is considered to be the relevant phase from the point of view of *in meso* crystallization. A perusal of the data in Table 1 and Fig. 5 shows that indeed the bulk of the screens are compatible with the cubic phase and accordingly, are likely to be useful in crystallization trials by the *in meso* method. However, in Table 1 are listed a variety of cubic phases which differ in space group type. These include the cubic-Ia3d, cubic-Pn3m, and cubic-Im3m phases. Representative cartoons of and diffraction patterns from the different cubics are presented in Fig. 1 and 4, respectively. Because the mechanism of *in meso* crystallization is unknown, and likewise the role of the cubic phase in the process, the significance of the cubic phase type cannot be evaluated. A careful study of crystallization from the different cubic phases has not yet been carried out, although both the cubic-Ia3d and the cubic-Pn3m have been seen to exist as phases from which membrane protein crystals eventually grow (P. Nollert, H. Qiu, M. Caffrey, J. Rosenbusch, E. Landau, unpublished data). To our knowledge, no such study involving the cubic-Im3m phase has been done. Our tentative recommendation, therefore, is that screens that produce cubic phases, regardless of type, are likely candidates for use in crystallization trials by the *in meso* method.

Cubic phase microstructure

The bulk of the screen solutions used in this study produce one of three different cubic phases when combined with monoolein. Within a cubic phase type, we see that the microstructure, or lattice size, changes depending on the screen composition (compare 2–42.1.20 and 2–4.1.20, for example). It also depends on temperature (compare 1–34.1.4 and 1–34.1.20, for example) and on the type of preparation used (compare 1–7.1.20 and 1–7.2.20, for example), as expected (Qiu and Caffrey, 2000). Unfortunately, due to the fact that the *in meso* method is in its infancy, the impact of mesophase microstructure on membrane protein crystallization has not been evaluated. Accordingly, it is not appropriate at this stage to make recommendations for or against a given screen based on the cubic phase lattice size it supports. However, given that a change in bilayer curvature (Chung and Caffrey, 1994a, 1994b) has been suggested as a driving force for crystal formation (Caffrey, 2000), it seems logical that lattice size will prove to be an important variable. Preliminary data on the crystallizability of bacteriorhodopsin *in meso* suggest that crystal formation occurs from the cubic-Pn3m phase when its lattice parameter has contracted to a limiting value (P. Nollert, H. Qiu, M. Caffrey, J. Rosenbusch, E. Landau, unpublished data). The

relevance of this to other proteins with membrane topologies different from that of bacteriorhodopsin is not known. The important point to note is that in addition to influencing phase type, the screen solution used can profoundly affect phase microstructure and that this may impact of the crystallization process.

CONCLUSIONS

The Hampton Screen and Screen 2 series of solutions have been evaluated for their compatibility with the hosting lipidic cubic phase which is integral to *in meso* membrane protein crystallization. Compatibility was evaluated in a monoolein-based cubic system at 4 and 20°C and under conditions mimicking two experimental protocols. One models a situation in which the cubic phase is in equilibrium with excess water (Prep. 1), and the other simulates the water-stressed condition (Prep. 2). Mesophase stability and phase microstructure were quantified by small-angle x-ray diffraction. Retention of the cubic phase in the presence of a given screen solution indicates that that screen is compatible with the *in meso* method for the conditions specified. The principal conclusions from this study follow.

- At 20°C, 90% of the 98 screen solutions examined produced the cubic phase under Prep. 1 conditions. This figure dropped to 50% when the Prep. 2 protocol was used.
- At 4°C, 50 to 60% of the screens were cubic phase compatible under Prep. 1 conditions. The number dropped to 25% under Prep. 2 conditions. At this low temperature, the cubic phase represents an undercooled or metastable state.
- Phase type and microstructure (lattice parameter) changed with sample screen content, screen composition, and temperature in ways that make good physicochemical sense.
- The sensitivity of phase type and microstructure just noted can be used in rationally designing the hosting mesophase for use in crystallizing new membrane proteins.

The widespread use of the *in meso* method in its present incarnation is compromised by low-temperature metastability. With monoolein as the hosting lipid, crystallization trials at temperatures below 20°C are precarious because the cubic phase so formed is unlikely to represent equilibrium. Thus, conversion to a non-cubic equilibrium phase during a trial is possible and such a conversion is potentially disastrous for the trial. The search continues for a lipid with properties similar to monoolein but which is stable in the cubic phase in the 0 to 25°C range.

Data deposition

Relevant data reported in this paper have been deposited in the Lipid Data Bank (http://www.ldb.chemistry.ohio-state.edu).

We thank Hampton Research Inc. for providing the screen solutions, T. Narayanan (beamline ID-2; ESRF, Grenoble, France) for technical support at the synchrotron, and the members of our research group for invaluable input on this project and for comments on the manuscript. The project was funded in part through grants DK45295, GM56969, and GM61070 from the National Institutes of Health, and grants DIR9016683 and DBI9981990 from the National Science Foundation. The use of Hampton Screen solutions in this study does not necessarily signify their endorsement by the authors.

REFERENCES

Ai, X., and M. Caffrey. 2000. Membrane protein crystallization in lipidic mesophases: detergent effect. *Biophys. J.* 79:394–405.

Briggs, J., H. Chung, and M. Caffrey. 1996. The temperature-composition phase diagram and mesophase structure characterization of the monoolein/water system. *J. Phys.* 6:723–751.

Caffrey, M. 1987. Kinetics and mechanism of transitions involving the lamellar, cubic, inverted hexagonal, and fluid isotropic phases of hydrated monoacylglycerides monitored by time-resolved x-ray diffraction. *Biochemistry* 26:6349–6363.

Caffrey, M. 2000. A lipid's eye view of membrane protein crystallization in mesophases. *Curr. Opin. Struct. Biol.* 10:486–497.

Cheng, A., B. Hummel, H. Qiu, and M. Caffrey. 1998. A simple mechanical mixer for small viscous lipid-containing samples. *Chem. Phys. Lipids.* 95:11–21.

Chung, H., and M. Caffrey. 1994a. The curvature elastic energy function of the cubic mesophase. *Nature* 368:224–226.

Chung, H., and M. Caffrey. 1994b. The neutral area surface in cubic mesophases. Location and properties. *Biophys. J.* 66:377–381.

Gerritsen, H., and M. Caffrey. 1990. Water transport in lyotropic liquid crystals and lipid-water systems: Mutual diffusion coefficient determination. *J. Phys. Chem.* 94:944–948.

Kolbe, M., H. Besir, L.-O. Essen, and D. Oesterhelt. 2000. Structure of the light-driven chloride pump halorhodopsin at 1.8 Å resolution. *Science.* 288:1390–1396.

Landau, E. M., and J. P. Rosenbusch. 1996. Lipidic cubic phases: a novel concept for the crystallization of membrane proteins. *Proc. Natl. Acad. Sci. U.S.A.* 93:14532–14535.

Larsson, K. 1994. Lipids: Molecular Organization, Physical Functions, and Technical Applications. The Oily Press Ltd. Dundee, Scotland.

Luecke, H., B. Schobert, H.-T. Richter, J.-P. Cartailler, and J. K. Lanyi. 1999. Structure of bacteriorhodopsin at 1.55 angstrom resolution. *J. Mol. Biol.* 291:899–911.

Luzzati, V. 1997. Biological significance of lipid polymorphism. The cubic phases. *Curr. Opin. Struct. Biol.* 5:661–668.

McPherson, A. 1999. Crystallization of Biological Macromolecules. Cold Spring Harbor Laboratory Press, New York.

Qiu, H., and M. Caffrey. 2000. Phase diagram of the monoolein/water system: Metastability and equilibrium aspects. *Biomaterials.* 21: 223–234.

Saas, H. J., G. Buldt, R. Gessenich, D. Hehn, D. Neff, R. Schlesinger, J. Berendzen, and P. Osmos. 2000. Structural alterations for proton translocation in the M state of wild-type bacteriorhodopsin. *Nature.* 406: 649–653.